ELSEVIER

www.elsevier.nl/locate/jorganchem

Journal of Organometallic Chemistry 606 (2000) 65–74

Journal of Organometallic Chemistry

Synthesis and reactivity of novel ruthenium carbene catalysts. X-ray structures of $[RuCl_2(=CHSC_6H_5)(P^iPr_3)_2]$ and $[RuCl_2(CHCH_2CH_2\text{-}C,N\text{-}2\text{-}C_5H_4N)(P^iPr_3)]$

Paul A. van der Schaaf *, Roman Kolly, Hans-Jürg Kirner, Francois Rime, Andreas Mühlebach, Andreas Hafner

Ciba Specialty Chemicals, CH-4002 Basel, Switzerland

Received 2 February 2000; received in revised form 27 April 2000

Abstract

Two novel classes of very air-stable ruthenium carbene complexes have been developed. The arylthio substituted ruthenium carbenes containing two bulky phosphines are deep purple solids, whereas the 2-pyridylethanyl substituted ruthenium carbene complexes contain only one bulky phosphine and are light-brown colored. One member of each class has been characterized with X-ray crystallography. The metathesis activity of these complexes has been investigated in the polymerization of dicyclopentadiene. Several excellent catalysts were identified. Desired geltimes and initiation temperatures could be easily tuned by changing the substitution pattern on the pendant ligand in the 2-pyridylethanyl substituted ruthenium carbenes.

Keywords: Ruthenium; Catalyst; Carbenes; Metathesis; ROMP; Dicyclopentadiene

1. Introduction

In the last years of the 2nd millennium, the use of ruthenium carbene catalysts for olefin metathesis reactions has dramatically increased in the field of organic and polymer chemistry. Primarily, this was caused by the development of well-defined ruthenium carbene catalysts by Grubbs group at CalTech [1]. Their pioneering work was followed by many others who 'fine-tuned' the catalyst system to increase stability and/or activity, improved catalyst syntheses, and, last but not least, incorporated the olefin metathesis chemistry in their strategies to develop novel synthetic routes to, or via classical routes not available, complex organic molecules [2].

Our long standing interest in olefin metathesis chemistry [3] led us to investigate the use of well-defined ruthenium carbene catalysts intensively. In this paper we describe two novel classes of ruthenium carbene catalysts and their first application in the polymerization of dicyclopentadiene (DCPD).

2. Results and discussion

2.1. Catalysts

Recently we published our first results on the solvent-free polymerization of DCPD using $[RuCl_2(p\text{-cymene})(PCy_3)]$ as catalyst precursor [3b]. With this one-component initiator, DCPD was polymerized in the presence of a wide variety of filler materials like quartz powder, alumina, and pigments to obtain materials with outstanding mechanical and electrical properties. Solutions of 0.3 wt% of this catalyst in DCPD are very latent, whereas upon raising the temperature to 80°C a fast and complete polymerization took place. We think that in the activation mechanism the *p*-cymene moiety is liberated and the 'half-naked' ruthenium is transformed into a more reactive ruthenium carbene complex. Most probably this transformation

* Corresponding author. Tel.: +41-61-6365433; fax: +41-61-6364011.

E-mail address: paul.van_der_schaaf@cibasc.com (P.A. van der Schaaf).

0022-328X/00/$ - see front matter
PII: S0022-328X(00)00289-8

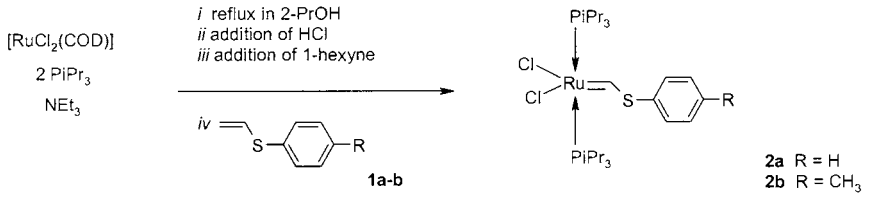

Scheme 1.

into a carbene is accelerated by the presence of some acetylenic impurities present in DCPD [4]. We could decrease the catalyst concentration significantly by using Grubbs' well-defined ruthenium carbene catalysts. However, the drawback of these highly reactive catalysts is the moderate latency. After solubilizing the catalyst in DCPD, the polymerization takes place almost immediately without any control of the rate of polymerization [5]. We tried to modify chemically this catalyst system in such a way that we could control the initiation rate of the polymerization. Surprisingly, we found that hetero atom substituted ruthenium carbenes [6] are also active catalysts for olefin metathesis reactions. Especially, arylsulfur substituted ruthenium carbenes appear to be very efficient catalysts [7]. This new class of catalysts can be easily prepared either via the reaction of Grubbs' benzylidene catalyst with an aryl vinyl thioether or via our one-pot procedure for the synthesis of ruthenium carbenes starting from [$RuCl_2$(1,5-cyclooctadiene)] via a ruthenium hydride species [8], see Scheme 1. In contrast to known procedures from the literature in which ruthenium hydrides are the key intermediates in the synthesis of ruthenium carbenes [9], this synthetic procedure generates a very reactive ruthenium hydride species in situ in boiling isopropanol without the use of hydrogen gas.

The catalysts **2a** and **2b** are purple, air-stable solids. By introducing the *para*-methyl group in **2b**, the solubility of the catalyst in apolar solvents, and dicyclopentadiene, was drastically increased. To elucidate the stereochemistry of these complexes an X-ray structure determination on **2a** was carried out. Suitable crystals were grown from a hot toluene solution. Fig. 1 shows the ORTEP drawing of **2a** together with the adopted numbering scheme. Selected bond distances and angles are given in Table 1.

Surprisingly, the presence of the sulfur atom on the carbene moiety does not significantly influence the structural properties of this carbene complex with respect to the crystal structure of the Grubbs benzylidene [1c]. This is also nicely reflected in the high metathesis activity of these compounds, see below. The activation mechanism of **2a** and **2b** is assumed to be similar to that for the ruthenium benzylidene complexes. This activation mechanism, as proposed by Grubbs et al. [10], is a dissociative mechanism in which one of the two phosphines dissociates from the ruthenium center

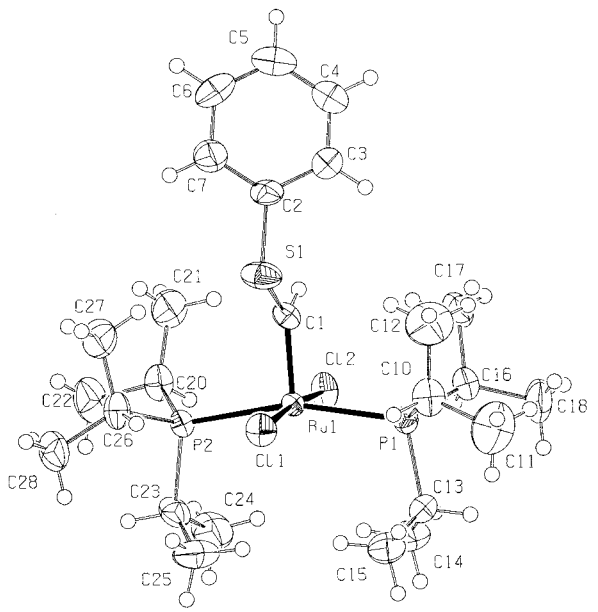

Fig. 1. ORTEP drawing of the molecular structure of [$RuCl_2$(=CHSPh)(P^iPr_3)$_2$] (**2a**) (thermal ellipsoids at 50% probability).

Table 1
Selected bond lengths (Å) and angles (°) for [$RuCl_2$(=CHSPh)(P^iPr_3)$_2$] (**2a**)

Bonds lengths	
Ru(1)–Cl(1)	2.3898(12)
Ru(1)–Cl(2)	2.3884(12)
Ru(1)–C(1)	1.837(4)
Ru(1)–P(1)	2.4196(10)
Ru(1)–P(2)	2.4184(11)
C(1)–S(1)	1.706(4)
S(1)–C(2)	1.782(4)
Bond angles	
Cl(1)–Ru(1)–Cl(2)	173.92(5)
P(1)–Ru(1)–P(2)	162.76(3)
Ru(1)–C(1)–S(1)	129.0(2)
C(1)–S(1)–C(2)	102.07(18)
P(1)–Ru(1)–C(1)	98.96(11)
P(2)–Ru(1)–C(1)	98.25(11)
Cl(1)–Ru(1)–C(1)	92.67(12)
Cl(2)–Ru(1)–C(1)	93.40(12)
P(1)–Ru(1)–Cl(1)	89.40(4)
P(1)–Ru(1)–Cl(2)	89.91(4)
P(2)–Ru(1)–Cl(1)	90.79(4)
P(2)–Ru(1)–Cl(2)	88.07(4)

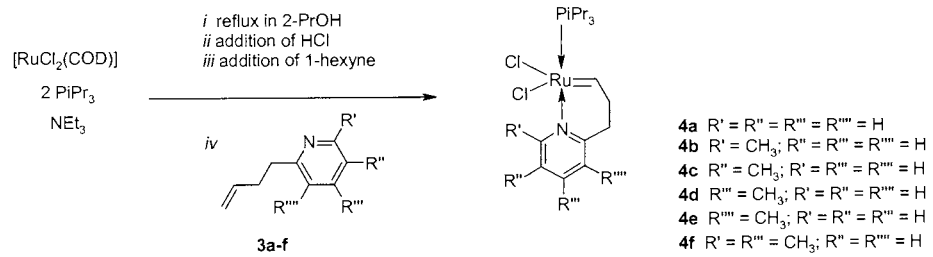

Scheme 2.

upon binding an olefin. Presumably the liberated phosphine remains in the proximity of the ruthenium center of coordinately unsaturated reactive intermediates. However, this reversible binding of the phosphine ligand also lowers the overall catalyst activity. Experimental evidence for the latter is provided by the fact that the addition of CuCl to capture liberated phosphine results in higher catalyst activity. Also the addition of acid to the reaction mixture produces an increased activity of the catalyst because of protonation of the free phosphine [11]. We approached this problem in a different way, and developed a new class of ruthenium carbene complexes in which a potentially coordinating ligand is directly bonded to the carbene moiety of the catalyst [12]. A very efficient group of catalysts are the 2-pyridylethanyl substituted ruthenium carbene complexes **4a**–**f**. Also this new class of catalyst can be easily prepared, either via the reaction of Grubbs benzylidene catalyst with a 2-(3-butenyl)pyridine or directly via our one-pot procedure for the synthesis of ruthenium carbenes starting from [$RuCl_2$(1,5-cyclooctadiene)] via a ruthenium hydride species, see Scheme 2.

These classes of catalysts are monophosphine complexes in which the carbene moiety is substituted with an intramolecularly coordinating pyridyl group [13]. The possibility of substitution of the pyridyl ring enabled us to fine-tune the reactivity of these catalysts, vide infra. The catalysts **4a**–**f** are light-brown, air-stable solids. To elucidate the stereochemistry of these complexes an X-ray structure determination of **4a** was carried out. Suitable crystals were grown from a hot toluene solution. Fig. 2 shows the ORTEP drawing of **4a** together with the adopted numbering scheme. Selected bond distances and angles are given in Table 2.

Again, the bond length of the ruthenium carbene moiety is closely related to that of Grubbs benzylidene catalyst and **2a**. The main difference of the structural properties of **4a** with the latter structures is the significant smaller Cl–Ru–Cl angle of 155°, which is probably a consequence of a combination of electronic and steric factors that accompany the formation of the six-membered chelate ring by replacing one bulky phosphine.

2.2. ROMP of DCPD

The metathesis activity of these new classes of catalysts has been tested on the polymerization of dicyclopentadiene (DCPD), see Scheme 3. In a first test we screened the activity of our catalysts in a differential

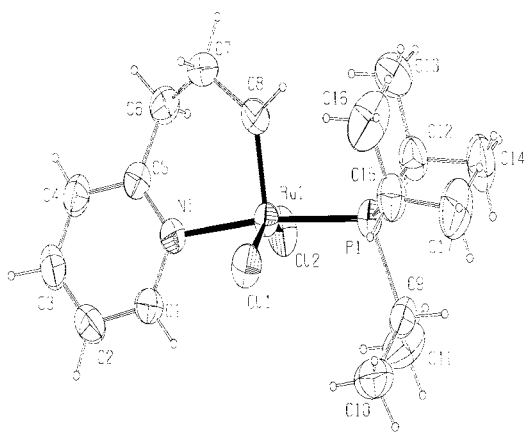

Fig. 2. ORTEP drawing of the molecular structure of [$RuCl_2$(=$CHCH_2CH_2$-*C*,*N*-2-C_5H_4N)(P^iPr_3)] (**4a**) (thermal ellipsoids at 50% probability).

Table 2
Selected bond lengths (Å) and angles (°) for [$RuCl_2$(=$CHCH_2CH_2$-*C*,*N*-2-C_5H_4N)(P^iPr_3)] (**4a**)

Bonds lengths	
Ru(1)–Cl(1)	2.3521(7)
Ru(1)–Cl(2)	2.3471(7)
Ru(1)–C(8)	1.810(3)
Ru(1)–P(1)	2.3423(7)
Ru(1)–N(1)	2.1542(19)
Bond angles	
Cl(1)–Ru(1)–Cl(2)	155.27(3)
P(1)–Ru(1)–N(1)	172.80(6)
Ru(1)–C(8)–C(7)	126.5(2)
P(1)–Ru(1)–C(8)	96.08(9)
N(1)–Ru(1)–C(8)	91.10(10)
Cl(1)–Ru(1)–C(8)	100.34(9)
Cl(2)–Ru(1)–C(8)	103.72(9)
P(1)–Ru(1)–Cl(1)	91.67(2)
P(1)–Ru(1)–Cl(2)	91.36(2)
N(1)–Ru(1)–Cl(1)	86.63(6)
N(1)–Ru(1)–Cl(2)	87.31(6)

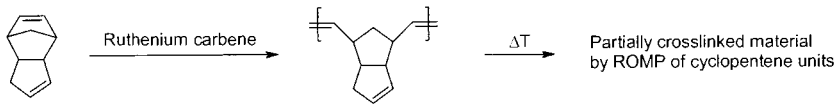

Scheme 3.

scanning calorimetry (DSC) apparatus. The results of this screening are given in Table 3.

These results clearly show that both arylthio substituted ruthenium carbenes **2a** and **2b** are very efficient initiators as well as the 2-pyridylethanyl substituted carbenes **4a**, **4b**, and **4f**. All of these catalysts gave poly(DCPD) with a glass transition temperature (T_g) far above 120°C (which indicates high conversions of $>98\%$). The vinyl substituted Grubbs catalyst **6** appeared to be a better initiator in this screening than the benzylidene catalyst **5**. These experiments also clearly show the very good latency of the 2-pyridylethanyl substituted ruthenium carbenes. Catalysts **4a**, **4b** and **4f** have all geltimes greater than 40 min. These high geltimes are needed for good handling of the DCPD/catalyst formulation.

The interesting candidates of this first screening were subsequently tested in a plate polymerization experiment. For this setup we used a heatable steel mold ($0.4 \times 30 \times 30$ cm). In an experiment a freshly prepared solution of the catalyst in DCPD ([DCPD]/[catalyst] = 4700:1) was poured into the preheated mold and the temperature was monitored. With this setup curing profiles and processing parameters were studied. Figs. 3 and 4 show the thermographs of the polymerization of DCPD initiated by **2a**, **2b**, and **4a**, **4b**, **4f**, respectively with a fixed mold temperature of 60°C.

The exotherms of the reactions with **2a** and **2b** are both higher than 180°C and the reactions are completed after ca. 1 min. With the catalysts **4b** and **4f** exotherms reach 165 and 178°C, respectively, and the reactions take ca. 2 min for completion. With catalyst **4a** no exotherm was measured and the DCPD was only slightly gelled after 4 min. However, by changing the initial mold temperature, the polymerization profiles changed drastically. Figs. 5–7 show the thermograph of the polymerization initiated by **2b**, **4a** and **4f**, respectively, at different mold temperatures (note: for a better comparison the y-axis shows the ΔT (°C) with respect to the mold temperature).

Fig. 5 clearly shows that a mold temperature of 50°C is not sufficient for the polymerization of DCPD initiated with **2b**, whereas with a mold temperature of 60°C, a high exotherm is observed with a peak maximum at 45 s. At higher mold temperatures the polymerization peak maximums of 20 s were reached (however, polymer properties like T_gs tend to decrease at very high polymerization rates). The optimum mold temperature for the polymerization initiated by **4a** appeared to be at ca. 90°C whereas this for **4f** is ca. 70°C, see Figs. 6 and 7.

3. Conclusion

Two novel classes of ruthenium carbene complexes have been prepared. Polymerization experiments show that these new ruthenium carbene complexes are excellent initiators for the solvent-free catalytic polymeriza-

Table 3
Results of the catalyst screening for the polymerization of DCPD [a]

Catalyst	T_g (°C) [b]	Gel time (min) [c]
2a	149	10
2b	142	12
4a	135	>60
4b	140	44
4c	102	>60
4d	No reaction	>60 (no reaction)
4e	78	>60
4f	149	51
5 [d]	68	2
6 [e]	147	3

[a] Experimental conditions. A solution of catalyst in 5 g DCPD was prepared and degassed in vacuum ([DCPD]/[catalyst] = 12 000:1). A sample of 20–30 mg of this solution was taken and a DSC scan was recorded (0–200°C with 10°C min^{-1}).

[b] The glass transition temperature (T_g) was determined in a second run.

[c] The gel time was determined as the time needed for the 5 g solution to flow like a honey.

[d] $[RuCl_2(=CHPh)(P^iPr_3)_2]$.

[e] $[RuCl_2(=CH–CH=CMe_2)(P^iPr_3)_2]$.

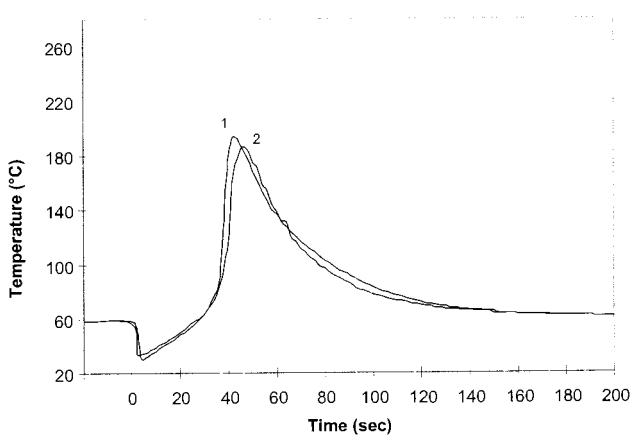

Fig. 3. Thermograph of the polymerization of DCPD with **2a** (1) and **2b** (2) at 60°C.

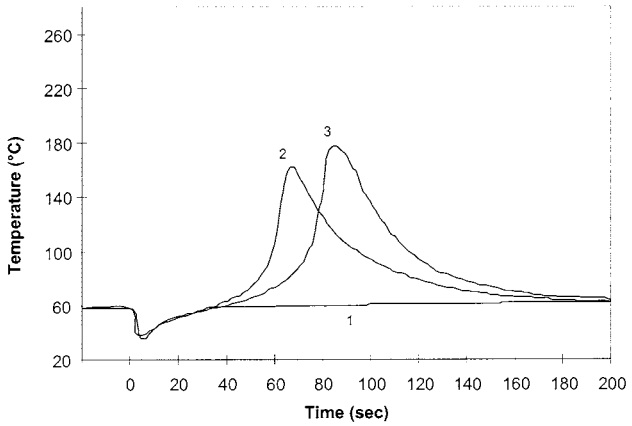

Fig. 4. Thermograph of the polymerization of DCPD with **4a** (1), **4b** (2) and **4f** (3) at 60°C.

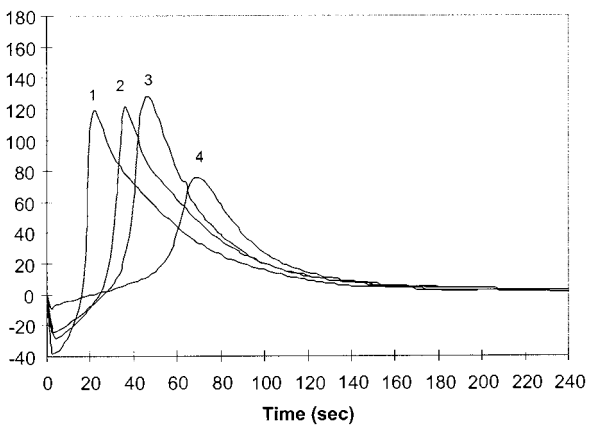

Fig. 5. Thermograph of the polymerization of DCPD with **2b** ([DCPD]/[catalyst] = 4700:1) at 80 (1), 70 (2), 60 (3) and 50°C (4).

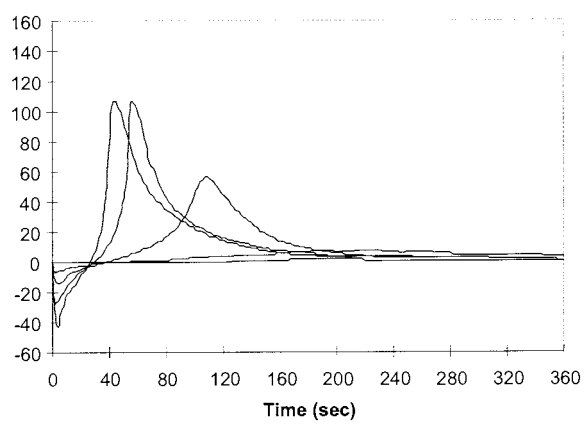

Fig. 6. Thermograph of the polymerization of DCPD with **4a** ([DCPD]/[catalyst] = 4700:1) at 100 (1), 90 (2), 80 (3), 70 (4) and 60°C (5).

tion of DCPD. We were able to perform so-called 'one-shot-full-cure' polymerizations in a preheated mold with polymerization times of less than 1 min. Desired geltimes and initiation temperatures can be tuned by changing the substitution pattern on the pendant ligand in the 2-pyridylethanyl substituted ruthenium carbenes. Experiments of using these novel catalysts in other applications are currently in progress.

4. Experimental

All reactions were carried out in an atmosphere of argon using standard Schlenk techniques when necessary. Solvents were used directly from the bottle (Fluka, puriss). Dicyclopentadiene was obtained from BF Goodrich (Ultrene 99) and liquefied with 3% MTD (methyl tetracyclododecene). Triisopropyl phosphine was prepared according to a known procedure [14]. All other chemicals were purchased from Fluka and used as supplied. Screening polymerization experiments were carried out in a DSC30 apparatus (differential scanning calorimetry) of Mettler Toledo equipped with a TC15 TA controller. Preparation of poly(DCPD) plates were performed in an in-house build, heatable mold ($0.4 \times 30 \times 30$ cm), with online temperature recording. ^{1}H- and ^{31}P-NMR spectra were recorded on a Bruker AC250 or AC300 spectrometer in $CDCl_3$ at 25°C. The X-ray crystal structure analyses were carried out by the BENEFRI-small molecule crystallography service, Institute of Chemistry, University of Neuchâtel, Switzerland (http://www.unine.ch/chim/chp2/smcs/SMCS.html).

4.1. Ligand synthesis

Ligand **1a** was prepared according to a modified literature procedure [15]. In this procedure thiophenol is deprotonated with sodium ethanolate, reacted with 1,2-dibromoethane, and dehydrobrominated with sodium ethanolate. Surprisingly, for the synthesis of **1b**, no desired product was obtained when the alkylation was performed with dibromoethane, followed by a de-

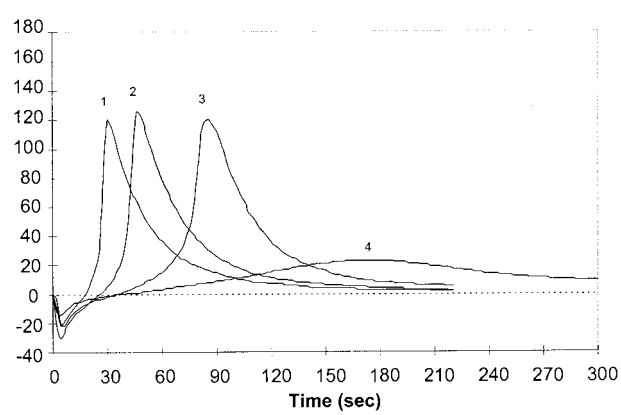

Fig. 7. Thermograph of the polymerization of DCPD with **4f** ([DCPD]/[catalyst] = 4700:1) at 80 (1), 70 (2), 60 (3) and 50°C (4).

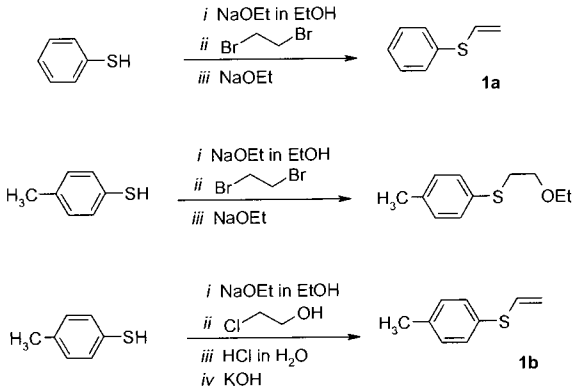

Scheme 4.

hydrobromination reaction. Instead, quantitative yields of (2-ethoxyethyl)-*para*-thiocresol were obtained. However, by using 2-chloroethanol as alkylating agent followed by reaction of HCl and dehydrochlorination, the product was obtained in good yield, see Scheme 4.

The 2-(3-butenyl)pyridines **3a**–**f** were synthesized according to a modified literature procedure [16]. All desired products were obtained in good yield when we deprotonated the *ortho*-methyl pyridines in THF at low-temperature (ca. −70°C) with butyl lithium, reacted the in situ formed lithiated species with allylbromide, warmed the reaction mixture to room temperature (r.t.) and then performed the work-up. However, such a reaction procedure is not economically feasible to perform on a larger scale. When we optimized the reaction procedure for 1a we performed the deprotonation with butyl lithium in THF at ca. 0°C and quenched the reaction with allyl chloride. After work-up the desired product was obtained with a good quality in 81% yield. However, when we used the same procedure for the preparation of **3f** a 60:40 mixture of the *para*- and *ortho*-alkylated product was obtained, see Scheme 5. Changing the solvent from THF to diethyl ether improved the selectivity of the deprotonation reaction dramatically [17], and the desired product was obtained in good quality in 79% yield.

4.2. Synthesis of **1a**

Thiophenol (110 g, 1 mol)) was added in small portions to a solution of sodium ethanolate (prepared by dissolving 23 g of sodium in 400 ml ethanol) over a period of 20 min. The resulting clear reaction mixture is then added dropwise, over a period of 2 h, to 1,2-dibromoethane (272 g, 1.4 mol) at r.t. After addition, the reaction mixture is allowed to stir an additional hour at r.t. A second solution of sodium ethanolate (prepared by dissolving 40 g sodium in 800 ml ethanol) was added dropwise over a period of 1 h. The resulting reaction mixture was heated to reflux overnight. The reaction mixture was then cooled to r.t. and filtered. The ethanol solution was concentrated in vacuum (60°C, 200 mbar), and was treated with 300 ml *tert*-butyl methyl ether and 200 ml water. The organic layer was separated, and the water layer was then extracted twice with *tert*-butyl methyl ether (2 × 50 ml). The combined organic layers were washed with a saturated aqueous sodium chloride solution (ca. 20%) until pH is neutral, and afterwards dried over magnesium sulfate. The organic layer was concentrated in vacuum, and the product was obtained pure by distillation (103°C, 40 mbar). The product was obtained in 46% yield (63 g) as a yellowish liquid [18]. Purity > 98% by GC. ^{1}H-NMR: δ 7.3 (5H, m, aryl-H); 6.53 (1H, C*H*=CH$_2$); 5.34 (2H, CH=C*H*$_2$).

4.3. Synthesis of **1b**

A 2.4 g of sodium (104 mmol), cut in small pieces, were added to 100 ml ethanol. After all sodium was

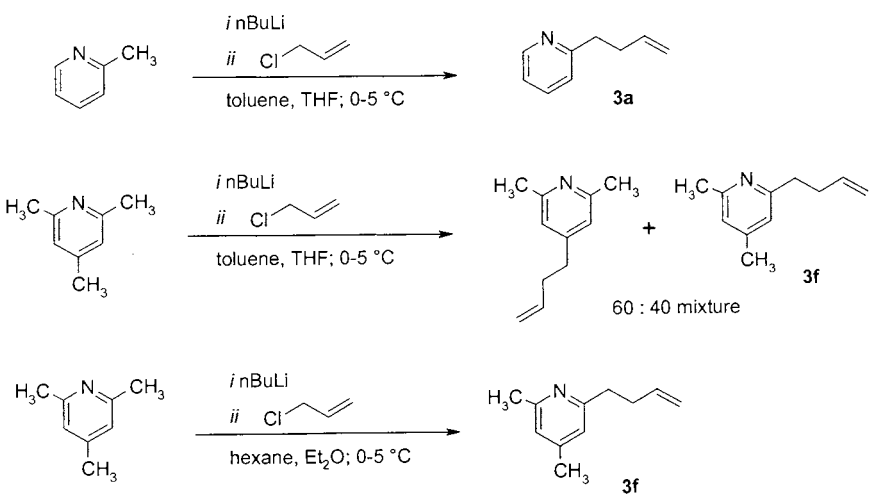

Scheme 5.

dissolved, *para*-thiocresol (12.4 g, 100 mmol) were added as a solid which rapidly dissolved. After 30 min stirring at r.t., 6.7 ml (100 mmol) 2-chloroethanol were added and the reaction mixture was heated to reflux for 3.5 h. During this step the reaction mixture went first opaque and then a white precipitate formed. The reaction mixture was cooled to r.t. and 60 ml fuming hydrogen chloride were added dropwise over a period of 10 min. The resulting reaction mixture was stirred for 15 h at r.t. and then heated to reflux for 4.5 h. The reaction mixture was then cooled to r.t. and diluted with 100 ml water. This mixture was extracted with *tert*-butyl methyl ether (7×40 ml). The combined organic phases were washed with 80 ml water, 80 ml of a 10% aqueous solution of NaOH, and 80 ml of a saturated aqueous solution of sodium chloride (ca. 20%), successively, and dried over sodium sulfate. After the solvents were removed in vacuum, the crude intermediate product was obtained as a yellow liquid in a quantitative yield (18.7 g). This product was used in the following steps without further purification.

A total of 18.7 g of crude intermediate were added to a 100 ml solution in ethanol containing 11.2 g of potassium hydroxide. The resulting reaction mixture was heated to reflux for 16 h, and a precipitate formed upon heating. After cooling the reaction mixture to r.t., it was filtered, and the filtercake was extracted with ethanol (3×30 ml). The combined ethanolic solutions were concentrated in vacuum to give the crude product as a yellow oil. After addition of some polymerization inhibitor [17], the product was purified by distillation (90–95°C, 18 mbar) giving the product as a colorless liquid in 53% yield. Purity $>98\%$ by GC. ^{1}H-NMR: δ 7.28 and 7.13 (4H, dd, aryl-H); 6.50 (1H, C*H*=CH_2); 5.26 (2H, CH=CH_2); 2.33 (3H, *para*-CH_3).

4.4. Synthesis of **2a**

A total of 2.5 g [$RuCl_2$(COD)] were suspended in 90 ml isopropanol (degassed to remove oxygen) 2.5 ml triethylamine and 3.6 ml P^iPr_3 were added, and then the reaction mixture was refluxed under argon for 3 h resulting in a clear, dark red solution. This red solution was cooled to -25°C and a light orange suspension formed. 17.8 ml of a 1.0 M HCl solution in diethyl ether were added in one portion (temperature raised to -17°C), and the reaction mixture was stirred for an additional 5 min keeping the temperature between -20 to -15°C. At -20°C 2.1 ml 1-hexyne were added in one portion (color became more brown). The reaction mixture was stirred for 1.5 h keeping the temperature between -20 and -15°C to yield a purple suspension. A total of 4.7 ml phenyl vinyl sulfide was then added and the temperature was raised to r.t. At this temperature the reaction mixture was stirred for an additional 30 min. The purple suspension was filtered and the fine purple solid was washed with methanol (3×10 ml), and dried in vacuum. This reaction procedure yielded 4.3 g pure product (78% yield). ^{1}H-NMR: δ 17.66 (s, 1, carbene-H); 7.4–7.1 (m, 5, SPh); 2.8 (m, 6, $P(CHMe_2)_3$); 1.2 (m, 36, $P(CHMe_2)_3$). ^{31}P-NMR: δ 42.3.

4.5. Synthesis of **2b**

The reaction was performed in a similar way as described for **2a**. Using *para*-tolyl vinyl sulfide (ligand **1b**), the desired product was obtained in 72% yield. ^{1}H-NMR: δ 17.62 (s, 1, carbene-H); 7.24 and 7.09 (dd, 4, SPh); 2.8 (m, 6, $P(CHMe_2)_3$); 2.28 (s, 3, *para*-Me); 1.2 (m, 36, $P(CHMe_2)_3$). ^{31}P-NMR: δ 42.2

4.6. Synthesis of **3a**

A total of 400 ml butyllithium (2.5 M sol. in toluene, 1 mol) was added dropwise over a period of 2.5 h to a cooled solution of 2-methylpyridine (93.13 g, 1 mol) in 320 ml THF of 0°C. The temperature of the reaction mixture was kept between 0 and 5°C during the addition of the butyllithium solution. After addition, the clear orange reaction mixture was stirred for an additional 30 min at 0°C. This orange reaction mixture was kept at 0°C and added dropwise over a period of 30 min to a cooled solution of allyl chloride (76.53 g, 1 mol) in 320 ml THF. During the addition of the organolithium intermediate, the temperature was kept between 0 and 5°C. After addition, the final reaction mixture was stirred for an additional 30 min. A total of 80 ml of isopropanol was added (to quench the remaining organolithium species) keeping the reaction mixture between 0 and 5°C. The reaction mixture, a yellow suspension, was warmed to r.t. and 320 ml of a saturated sodium chloride solution in water (ca. 20 wt%) were added. The resulting suspension was filtered over Celite®, and the filtercake was extracted with *tert*-butyl methyl ether (3×200 ml). The organic phase was separated from the combined reaction mixture with the ethereal washings and dried over sodium sulfate. The organic phase was concentrated in vacuo giving the crude product. The product was purified by distillation (42–50°C, 0.015 mbar), and obtained as a colorless liquid in 81% yield (108 g). Purity: $>98\%$ (GC). ^{1}H-NMR: δ 8.50, 7.54 and 7.07 (4, py-H); 5.84 (1, CH_2CH_2CH=CH_2); 4.97 (2, CH_2CH_2CH=CH_2); 2.85 (CH_2CH_2CH=CH_2); 2.44 (2, CH_2CH_2CH=CH_2).

4.7. Synthesis of **3b**

The reaction was performed in a similar way as described for **3a**. Starting from 2,6-dimethyl pyridine, the product was obtained after distillation (29–31°C, 0.013 mbar) in 80% yield with a purity of $>97\%$ by

GC. ^{1}H-NMR: δ 7.44 and 6.90 (3, py-H); 5.82 (1, $CH_2CH_2CH{=}CH_2$); 4.97 (2, $CH_2CH_2CH{=}CH_2$); 2.81 (2, $CH_2CH_2CH{=}CH_2$); 2.49 (3, 6-Me py); 2.41 (2, $CH_2CH_2CH{=}CH_2$).

4.8. Synthesis of **3c**

The reaction was performed in a similar way as described for **3a**, however, the lithiation and alkylation with allylbromide were performed in diethyl ether at −70°C. Starting from 2,5-dimethylpyridine, the product was obtained after flash distillation in 65% yield with a purity of >95% by GC. ^{1}H-NMR: δ 8.23, 7.26 and 6.90 (3, py-H); 5.74 (1, $CH_2CH_2CH{=}CH_2$); 4.88 (2, $CH_2CH_2CH{=}CH_2$); 2.70 (2, $CH_2CH_2CH{=}CH_2$); 2.38 (2, $CH_2CH_2CH{=}CH_2$); 2.16 (3, 5-Me py).

4.9. Synthesis of **3d**

The reaction was performed in a similar way as described for **3c**. Starting with 2,4-dimethyl pyridine, the product was obtained in 72% yield with a purity of >95% by GC. ^{1}H-NMR: δ 8.33, 6.92 and 6.88 (3, py-H); 5.82 (1, $CH_2CH_2CH{=}CH_2$); 5.00 (2, $CH_2CH_2CH{=}CH_2$); 2.79 (2, $CH_2CH_2CH{=}CH_2$); 2.41 (2, $CH_2CH_2CH{=}CH_2$); 2.27 (3, 4-Me py).

4.10. Synthesis of **3e**

The reaction was performed in a similar way as described for **3c**. Starting with 2,3-dimethyl pyridine, the product was obtained in 62% yield with a purity of >95% by GC. ^{1}H-NMR: δ 8.25, 7.27 and 6.90 (3, py-H); 5.80 (1, $CH_2CH_2CH{=}CH_2$); 4.88 (2, $CH_2CH_2CH{=}CH_2$); 2.76 (2, $CH_2CH_2CH{=}CH_2$); 2.36 (2, $CH_2CH_2CH{=}CH_2$); 2.18 (3, 3-Me py).

4.11. Synthesis of **3f**

A total of 200 ml butyllithium (1.6 M solution in hexane, 0.32 mol) was added dropwise over a period of 80 min to a cooled solution of 2,4,6-trimethylpyridine (38.8 g, 0.32 mol) in 250 ml diethyl ether at 0°C. The temperature of the reaction mixture was kept between 0 and 5°C during the addition of the butyllithium solution. After addition, the clear orange solution was stirred for an additional hour at 0°C.

This orange reaction mixture was kept at 0°C and added over a period of 15 min to a cooled solution of allyl chloride (25.0 g, 0.32 mol) in 100 ml diethyl ether of 0°C. During the addition of the pyridylmethyl lithium reaction mixture, the temperature was kept between 0 and 5°C. After addition, the final reaction mixture was stirred for an additional hour at this temperature. A total of 30 ml of isopropanol were added (to quench the remaining alkyllithium species) keeping the reaction mixture between 0 and 5°C. The reaction mixture, a yellow suspension, was warmed to r.t. and 150 ml of a saturated sodium chloride solution in water (ca. 20 wt%) were added. The resulting suspension was filtered over Celite®, and the organic phase was separated. The filtercake was extracted with *tert*-butyl methyl ether (3 × 100 ml). The combined organic phase was dried over sodium sulfate. The organic phase was concentrated in vacuo giving the crude product. The product was purified by distillation (42–45°C, 0.02 mbar), and obtained as a colorless liquid in 79% yield (41 g). Purity: >95% by GC (contains ca. 3% *sym*-collidine). ^{1}H-NMR: δ 6.75 (2, py-H); 5.84 (1, $CH_2CH_2CH{=}CH_2$); 4.99 (2, $CH_2CH_2CH{=}CH_2$); 2.77 (2, $CH_2CH_2CH{=}CH_2$); 2.45 (2, $CH_2CH_2CH{=}CH_2$); 2.45 (3, 6-CH_3 py); 2.24 (3, 4-CH_3 py).

4.12. Synthesis of **4a**

A total of 4.4 g [$RuCl_2$(COD)] were suspended in 150 ml isopropanol, degassed to remove oxygen, 4.4 ml triethylamine and 6.4 ml P^{i}Pr$_3$ were then added. The reaction mixture was refluxed under argon for 3 h resulting in a clear, dark-red solution. This red solution was cooled to −20°C to yield a light-orange suspension. A total of 31.5 ml of a 1.0 M HCl solution in diethyl ether were added over a period of 15 min, and the reaction mixture was stirred for an additional 15 min keeping the temperature between −20 and −15°C. A total of 6.2 ml of 1-hexyne were added in one portion at −20°C (color changed to brown). The reaction mixture was stirred for 1.5 h keeping the temperature between −20 and −15°C leading to a purple suspension. A total of 2.7 g 2-(3-butenyl)pyridine were added at −15°C. The temperature was slowly raised to r.t. and the reaction mixture was stirred for an additional 2 h. The brown colored suspension was concentrated in vacuum leaving a brownish crude product. Stirring the crude product with 20 ml chilled methanol gave a brown suspension. This suspension was filtered and a fine brown powder was obtained as the product. This product was washed with chilled methanol (3 × 10 ml), and dried in vacuum. This procedure yielded 4.8 g of pure product (yield 68%). ^{1}H-NMR: δ 19.41 (dt, 1, carbene-H, $^3J_{PH}$ = 11.7 Hz); 8.70, 7.58, 7.19 (4, py-H); 3.60 (m, 2, $=CHCH_2CH_2$); 2.5 (m, 5, $=CHCH_2CH_2$ and P(CHMe$_2$)$_3$); 1.4 (m, 18, P(CHMe_2)$_3$). ^{31}P-NMR: δ 44.3.

4.13. Synthesis of **4b**

The reaction was performed in a similar way as described for **4a**. Using 2-(3-butenyl)-6-methylpyridine (ligand **3b**) the desired product was obtained as a light-brown powder in 65% yield. ^{1}H-NMR: δ 19.77 (dt, 1, carbene-H, $^3J_{PH}$ = 13.0 Hz); 7.50, 7.04 (3, py-H);

3.40 (m, 2, =CHCH$_2$*CH$_2$*); 3.22 (s, 3, 6-methyl); 2.93 (m, 2, =CH*CH$_2$*CH$_2$); 2.65 (m, 3, P(C*H*Me$_2$)$_3$); 1.4 (m, 18, P(CH*Me$_2$*)$_3$). ^{31}P-NMR: δ 42.5.

4.14. Synthesis of **4c**

The reaction was performed in a similar way as described for **4a**. Using 2-(3-butenyl)-5-methylpyridine (ligand **3c**) the desired product was obtained as a brown powder in 61% yield. ^{1}H-NMR: δ 19.44 (dt, 1, carbene-H, $^3J_{PH} = 11.9$ Hz); 8.47, 7.40, 7.08 (3, py-H); 3.53 (m, 2, =CHCH$_2$*CH$_2$*); 2.50 (m, 3, P(C*H*Me$_2$)$_3$); 2.39 (m, 2, =CH*CH$_2$*CH$_2$); 2.26 (s, 3, 5-methyl); 1.4 (m, 18, P(CH*Me$_2$*)$_3$). ^{31}P-NMR: δ 44.0.

4.15. Synthesis of **4d**

The reaction was performed in a similar way as described for **4a**. Using 2-(3-butenyl)-4-methylpyridine (ligand **3d**) the desired product was obtained as a brown powder in 65% yield. ^{1}H-NMR: δ 19.48 (dt, 1, carbene-H, $^3J_{PH} = 11.8$ Hz); 8.57, 7.24, 7.07 (3, py-H); 3.53 (m, 2, =CHCH$_2$*CH$_2$*); 2.60 (m, 3, P(C*H*Me$_2$)$_3$); 2.46 (m, 2, =CH*CH$_2$*CH$_2$); 2.36 (s, 3, 4-methyl); 1.4 (m, 18, P(CH*Me$_2$*)$_3$). ^{31}P-NMR: δ 42.8.

4.16. Synthesis of **4e**

The reaction was performed in a similar way as described for **4a**. Using 2-(3-butenyl)-3-methylpyridine (ligand **3e**) the desired product was obtained as a brown powder in 60% yield. ^{1}H-NMR: δ 19.45 (dt, 1, carbene-H, $^3J_{PH} = 11.5$ Hz); 8.58, 7.44, 7.08 (3, py-H); 3.53 (m, 2, =CHCH$_2$*CH$_2$*); 2.97 (m, 2, =CH*CH$_2$*CH$_2$); 2.55 (m, 3, P(C*H*Me$_2$)$_3$); 2.34 (s, 3, 3-methyl); 1.4 (m, 18, P(CH*Me$_2$*)$_3$). ^{31}P-NMR: δ 44.6.

4.17. Synthesis of **4f**

The reaction was performed in a similar way as described for **4a**. Using 2-(3-butenyl)-5-methylpyridine (ligand **3f**) the desired product was obtained as a brown powder in 55% yield. ^{1}H-NMR: δ 19.75 (dt, 1, carbene-H, $^3J_{PH} = 13.1$ Hz); 6.85, 6.82 (2s, 2, py-H); 3.29 (m, 2, =CHCH$_2$*CH$_2$*); 3.11 (s, 3, 6-methyl); 2.86 (m, 2, =CH*CH$_2$*CH$_2$); 2.61 (m, 3, P(C*H*Me$_2$)$_3$); 2.24 (s, 3, 4-methyl); 1.4 (m, 18, P(CH*Me$_2$*)$_3$). ^{31}P-NMR: δ 42.3

4.18. Crystal structure of **2a**

Suitable crystals of **2a** were grown from a hot toluene solution as very small dark-red rods. $C_{25}H_{48}Cl_2P_2RuS$, triclinic, space group, $P\bar{1}$, $a = 8.7596(7)$, $b = 9.7255(9)$, $c = 18.7729(18)$ Å, $\alpha = 76.75(1)$, $\beta = 81.61(1)$, $\gamma = 75.19(1)°$, $V = 1498.5(2)$ Å^3, $Z = 2$, $D_{calc} = 1.362$ g cm^{-3}, 11 668 reflections collected, 5358 independent reflections ($R_{int} = 0.063$), 3116 were considered observed [$I > 2\sigma(I)$], final $R = 0.0341$, $wR_2 = 0.0476$ (observed data), goodness of fit 0.698, residual density max./min. 0.341 (near the Ru atom) / −0.340 e Å^{-3}. Absorption coefficient $\mu = 0.802$ mm^{-1}; no correction for absorption was applied. Intensity data were collected at r.t. on a Stoe image plate diffraction system using Mo Kα graphite monochromated radiation. Image plate distance 70 mm, ϕ scans 0–200°, step $\Delta\phi = 1°$, 2θ range 3.27–52.1°, d_{max}–$d_{min} = 12.45$–0.8 1 Å. The structure was solved by direct methods using the program SHELXS-97 [19]. The refinement and all further calculations were carried out using SHELXL-97 [20]. All of the H-atoms were included in calculated positions and treated as riding atoms using SHELXL-97 default parameters. The non-H atoms were refined anisotropically, using weighted full-matrix least-squares on F^2.

4.19. Crystal structure of **4a**

Suitable crystals of **4a** were grown from a hot toluene solution as dark red blocks. $C_{17}H_{30}Cl_2NPRu$, triclinic, space group, $P\bar{1}$ $a = 8.2949(5)$, $b = 8.8564(5)$, $c = 15.7133(8)$ Å, $\alpha = 92.908(4)$, $\beta = 102.328(6)$, $\gamma = 114.821(5)°$, $Z = 2$, $D_{calc} = 1.483$ g cm^{-3}, 6805 reflections collected, 3754 independent reflections ($R_{int} = 0.0249$), 3412 were considered observed [$I > 2\sigma(I)$], final $R = 0.0249$, $wR_2 = 0.0567$ (observed data), goodness of fit 1.101, residual density max./min. 0.373/ −0.379 e Å^{-3}. Absorption coefficient $\mu = 1.116$ mm^{-1}; no correction for absorption was applied. Intensity data were collected at r.t. on a Stoe AED2 4-circle diffractometer using Mo Kα graphite monochromated radiation, using $2\theta/\omega$ scans in the range 4–51° in 2θ. The structure was solved by direct methods using the program SHELXS-97 [19]. The refinement and all further calculations were carried out using SHELXL-97 [20]. The H-atoms of the organic ligand were located from difference maps and refined isotropically. The H-atoms of the tris(isopropyl)phosphine ligand were included in calculated positions and treated as riding atoms using SHELXL-97 default parameters. The non-H atoms were refined anisotropically, using weighted full-matrix least-squares on F^2.

5. Supplementary material

The crystallographic CIF files have been deposited with the Cambridge Crystallographic Data Center (deposition numbers: CCDC 138602 (**2a**); CCDC 138603 (**4a**)). Copies of this information may be obtained free of charge from: The Director, CCDC, 12 Union Road, Cambridge, CB2 1EZ, UK (Fax: +44-1223-336-033; e-mail: deposit@ccdc.cam.ac.uk or www: http://www.ccdc.cam.ac.uk).

References

[1] (a) S.T. Nguyen, L.K. Johnson, R.H. Grubbs, J.W. Ziller, J. Am. Chem. Soc. 114 (1992) 3974. (b) P. Schwab, M.B. France, J.W. Ziller, R.H. Grubbs, Angew. Chem. Int. Ed. Engl. 34 (1995) 2039. (c) P. Schwab, R.H. Grubbs, J.W. Ziller, J. Am. Chem. Soc. 118 (1996) 100.

[2] (a) D.L. Wright, Curr. Org. Chem. 3 (1998) 211. (b) A.H. Hoveyda, Top. Organomet. Chem. 1 (1998) 105. (c) M.L. Randall, M.L. Snapper, J. Mol. Catal. A: Chem. 133 (1998) 29. (d) R.H. Grubbs, S. Chang, Tetrahedron 54 (1998) 4413. (e) H.E. Blackwell, D.J. O'Leary, A.K. Chatterjee, R.A. Washenfelder, D.A. Bussmann, R.H. Grubbs, J. Am. Chem. Soc. 122 (2000) 58.

[3] (a) A. Mühlebach, P.A. van der Schaaf, A. Hafner, F. Setiabudi, J. Mol. Catal. A: Chem. 132 (1998) 181. (b) A. Hafner, A. Mühlebach, P.A. van der Schaaf, Angew. Chem. Int. Ed. Engl. 36 (1997) 2121. (c) P.A. van der Schaaf, A. Hafner, A. Mühlebach, Angew. Chem. Int. Ed. Engl. 35 (1996) 1845. (e) A. Hafner, P.A. van der Schaaf, A. Mühlebach, Chimia 50 (1996) 131.

[4] A. Mühlebach, P.A. van der Schaaf, A. Hafner, Patent EP 844,263.

[5] A patent has been filed using triphenyl phosphine as gel modification agent: C.S. Woodson Jr., R.H. Grubbs, Patent WO 97/20865.

[6] From the literature it was known that PPh_3 containing hetero atom substituted ruthenium carbenes are inactive in olefin metathesis reactions: Z. Wu, S.T. Nguyen, R.H. Grubbs, J.W. Ziller, J. Am. Chem. Soc. 117 (1995) 5503.

[7] P.A. van der Schaaf, A. Mühlebach, A. Hafner, Patent WO 99/00396.

[8] P.A. van der Schaaf, R. Kolly, A. Hafner, J. Chem. Soc. Chem. Commun. (2000) 1045.

[9] (a) J.N. Coalter III, G.J. Spivak, H. Gerard, E. Clot, E.R. Davidson, O. Eisenstein, K.G. Caulton, J. Am. Chem. Soc. 120 (1998) 9388. (b) T.E. Wilhelm, T.R. Beldarrain, S.N. Brown, R.H. Grubbs, Organometallics 16 (1997) 3867. (c) T.R. Beldarrain, R.H. Grubbs, Organometallics 16 (1997) 4001. (d) C. Grünwald, O. Gevert, J. Wolf, P. Gonzalez-Herrero, H. Werner, Organometallics 15 (1996) 1960. (e) J. Wolf, W. Stüer, C. Grünwald, H. Werner, P. Schwab, M. Schulz, Angew. Chem. Int. Ed. Engl. 37 (1998) 1124.

[10] E.L. Dias, S.T. Nguyen, R.H. Grubbs, J. Am. Chem. Soc. 119 (1997) 3887.

[11] (a) D.M. Lynn, B. Mohr, R.H. Grubbs, Polym. Prepr. 39 (1998) 278. (b) D.M. Lynn, B. Mohr, R.H. Grubbs, J. Am. Chem. Soc. 120 (1998) 1627. (c) D.M. Lynn, E.L. Dias, R.H. Grubbs, B. Mohr, Patent WO 99/22865.

[12] P.A. van der Schaaf, A. Mühlebach, A. Hafner, Patent WO 99/00397.

[13] Another approach of an intramolecularly coordinating ligand using a bidentate Schiff-base ligand has been published recently: S. Chang, L. Jones II, C. Wang, L.M. Henling, R.H. Grubbs, Organometallics 17 (1998) 3460.

[14] H.J. Lorenz, A.R. Zintl, V. Franzen, Patent US 3,499,039.

[15] L.E. Paquette, R.V.C. Carr, Org. Synth. 64 (1986) 157.

[16] (a) J. Chengebroyen, M. Grellier, M. Pfeffer, Eur. J. Inorg. Chem. (1998) 1563. (b) B.T. Heaton, D.J.A. McCaffrey, J. Chem. Soc. Dalton Trans. (1979) 1078. (c) M. Israeli, D.K. Laing, L.D. Pettit, J. Chem. Soc. Dalton Trans. (1974) 2194. (d) W.A. Ayer, K. Piers, Can. J. Chem. 45 (1967) 451.

[17] (a) E.M. Kaiser, Tetrahedron 39 (1983) 2055. (b) K. Takahashi, K. Konishi, M. Ushio, M. Takaki, R. Asami, J. Organomet. Chem. 50 (1973) 1. (c) E. Kaiser, G.J. Bartling, W.R. Thomas, S.B. Nichols, D.R. Nash, J. Org. Chem. 38 (1973) 71.

[18] The yield of the synthesis can be increased when some radical scavenger, like 4-hydroxy-2,2,6,6-tetramethylpiperidine-1-oxy radical (4-hydroxy-TEMPO = PROSTAB™ 5198 of Ciba Specialty Chemicals), is added to the crude product before distillation to prevent polymerization. It is advisable to add also some stabilizer when the product has to be stored for longer periods of time.

[19] G.M. Sheldrick, Acta Crystallogr. Sect. A 46 (1990) 467.

[20] G.M. Sheldrick, SHELXL-97, Universität Göttingen, Göttingen, Germany, 1999.